

A Study of $J/\psi \rightarrow \gamma\gamma V(\rho, \phi)$ Decays with the BESII Detector

J. Z. Bai¹, Y. Ban¹⁰, J. G. Bian¹, X. Cai¹, J. F. Chang¹, H. F. Chen¹⁵,
 H. S. Chen¹, H. X. Chen¹, J. C. Chen¹, Jin Chen¹, Jun Chen⁶, M. L. Chen¹,
 Y. B. Chen¹, S. P. Chi¹, Y. P. Chu¹, X. Z. Cui¹, H. L. Dai¹, Y. S. Dai¹⁷,
 Z. Y. Deng¹, L. Y. Dong¹, S. X. Du¹, Z. Z. Du¹, J. Fang¹, S. S. Fang¹, C. D. Fu¹,
 H. Y. Fu¹, L. P. Fu⁶, C. S. Gao¹, M. L. Gao¹, Y. N. Gao¹⁴, M. Y. Gong¹,
 W. X. Gong¹, S. D. Gu¹, Y. N. Guo¹, Y. Q. Guo¹, S. W. Han¹, J. He¹, K. L. He¹,
 M. He¹¹, X. He¹, Y. K. Heng¹, H. M. Hu¹, T. Hu¹, G. S. Huang¹, L. Huang⁶,
 X. P. Huang¹, X. B. Ji¹, Q. Y. Jia¹⁰, C. H. Jiang¹, X. S. Jiang¹, D. P. Jin¹,
 S. Jin¹, Y. Jin¹, Y. F. Lai¹, F. Li¹, G. Li¹, H. H. Li¹, J. Li¹, J. C. Li¹, Q. J. Li¹,
 R. B. Li¹, R. Y. Li¹, S. M. Li¹, W. Li¹, W. G. Li¹, X. L. Li⁷, X. Q. Li⁹, X. S. Li¹⁴,
 Y. F. Liang¹³, H. B. Liao⁵, C. X. Liu¹, Fang Liu¹⁵, F. Liu⁵, H. M. Liu¹, J. B. Liu¹,
 J. P. Liu¹⁶, R. G. Liu¹, Y. Liu¹, Z. A. Liu¹, Z. X. Liu¹, G. R. Lu⁴, F. Lu¹,
 J. G. Lu¹, C. L. Luo⁸, X. L. Luo¹, F. C. Ma⁷, J. M. Ma¹, L. L. Ma¹¹, X. Y. Ma¹,
 Z. P. Mao¹, X. C. Meng¹, X. H. Mo¹, J. Nie¹, Z. D. Nie¹, H. P. Peng¹⁵, N. D. Qi¹,
 C. D. Qian¹², H. Qin⁸, J. F. Qiu¹, Z. Y. Ren¹, G. Rong¹, L. Y. Shan¹, L. Shang¹,
 D. L. Shen¹, X. Y. Shen¹, H. Y. Sheng¹, F. Shi¹, X. Shi¹⁰, L. W. Song¹,
 H. S. Sun¹, S. S. Sun¹⁵, Y. Z. Sun¹, Z. J. Sun¹, X. Tang¹, N. Tao¹⁵, Y. R. Tian¹⁴,
 G. L. Tong¹, D. Y. Wang¹, J. Z. Wang¹, L. Wang¹, L. S. Wang¹, M. Wang¹, Meng
 Wang¹, P. Wang¹, P. L. Wang¹, S. Z. Wang¹, W. F. Wang¹, Y. F. Wang¹,
 Zhe Wang¹, Z. Wang¹, Zheng Wang¹, Z. Y. Wang¹, C. L. Wei¹, N. Wu¹,
 Y. M. Wu¹, X. M. Xia¹, X. X. Xie¹, B. Xin⁷, G. F. Xu¹, H. Xu¹, Y. Xu¹,
 S. T. Xue¹, M. L. Yan¹⁵, W. B. Yan¹, F. Yang⁹, H. X. Yang¹⁴, J. Yang¹⁵,
 S. D. Yang¹, Y. X. Yang³, L. H. Yi⁶, Z. Y. Yi¹, M. Ye¹, M. H. Ye², Y. X. Ye¹⁵,
 C. S. Yu¹, G. W. Yu¹, C. Z. Yuan¹, J. M. Yuan¹, Y. Yuan¹, Q. Yue¹, S. L. Zang¹,
 Y. Zeng⁶, B. X. Zhang¹, B. Y. Zhang¹, C. C. Zhang¹, D. H. Zhang¹, H. Y. Zhang¹,
 J. Zhang¹, J. M. Zhang⁴, J. Y. Zhang¹, J. W. Zhang¹, L. S. Zhang¹, Q. J. Zhang¹,
 S. Q. Zhang¹, X. M. Zhang¹, X. Y. Zhang¹¹, Yiyun Zhang¹³, Y. J. Zhang¹⁰,
 Y. Y. Zhang¹, Z. P. Zhang¹⁵, Z. Q. Zhang⁴, D. X. Zhao¹, J. B. Zhao¹,
 J. W. Zhao¹, P. P. Zhao¹, W. R. Zhao¹, X. J. Zhao¹, Y. B. Zhao¹, Z. G. Zhao^{1*},
 H. Q. Zheng¹⁰, J. P. Zheng¹, L. S. Zheng¹, Z. P. Zheng¹, X. C. Zhong¹,
 B. Q. Zhou¹, G. M. Zhou¹, L. Zhou¹, N. F. Zhou¹, K. J. Zhu¹, Q. M. Zhu¹,
 Yingchun Zhu¹, Y. C. Zhu¹, Y. S. Zhu¹, Z. A. Zhu¹, B. A. Zhuang¹, B. S. Zou¹.

(BES Collaboration)

¹ Institute of High Energy Physics, Beijing 100039, People's Republic of China

² China Center of Advanced Science and Technology, Beijing 100080, People's Republic of China

³ Guangxi Normal University, Guilin 541004, People's Republic of China

⁴ Henan Normal University, Xinxiang 453002, People's Republic of China

⁵ Huazhong Normal University, Wuhan 430079, People's Republic of China

⁶ Hunan University, Changsha 410082, People's Republic of China

- ⁷ Liaoning University, Shenyang 110036, People's Republic of China
⁸ Nanjing Normal University, Nanjing 210097, People's Republic of China
⁹ Nankai University, Tianjin 300071, People's Republic of China
¹⁰ Peking University, Beijing 100871, People's Republic of China
¹¹ Shandong University, Jinan 250100, People's Republic of China
¹² Shanghai Jiaotong University, Shanghai 200030, People's Republic of China
¹³ Sichuan University, Chengdu 610064, People's Republic of China
¹⁴ Tsinghua University, Beijing 100084, People's Republic of China
¹⁵ University of Science and Technology of China, Hefei 230026, People's Republic of China
¹⁶ Wuhan University, Wuhan 430072, People's Republic of China
¹⁷ Zhejiang University, Hangzhou 310028, People's Republic of China
- * Visiting professor to University of Michigan, Ann Arbor, MI 48109 USA

Abstract

Using a sample of 58×10^6 J/ψ events collected with the BESII detector, radiative decays $J/\psi \rightarrow \gamma\gamma V$, where $V = \rho$ or ϕ , are studied. A resonance around 1420 MeV/ c^2 ($X(1424)$) is observed in the $\gamma\rho$ mass spectrum. Its mass and width are measured to be 1424 ± 10 (stat) ± 11 (sys) MeV/ c^2 and $101.0 \pm 8.8 \pm 8.8$ MeV/ c^2 , respectively, and its branching ratio $B(J/\psi \rightarrow \gamma X(1424) \rightarrow \gamma\gamma\rho)$ is determined to be $(1.07 \pm 0.17 \pm 0.11) \times 10^{-4}$. A search for $X(1424) \rightarrow \gamma\phi$ yields a 95% C.L. upper limit $B(J/\psi \rightarrow \gamma X(1424) \rightarrow \gamma\gamma\phi) < 0.82 \times 10^{-4}$.

Key words: J/ψ , Resonance, Meson, Glueball

PACS: 13.25.Gv, 14.40.Gx, 13.40.Hq.

1 Introduction

Experimentally the structure of the $\eta(1440)$ remains unresolved. The existence of two overlapping pseudo-scalar states has been suggested: one around 1410 MeV/ c^2 decays into both $K\bar{K}\pi$ and $\eta\pi\pi$, and the other around 1470 MeV/ c^2 decays only to $K\bar{K}\pi$ [1,2]. It is therefore conceivable that the higher mass state is the $s\bar{s}$ member of the 2^1S_0 nonet [3], while the lower mass state may contain a large gluonic content [4].

Standard perturbative theory predicts [5] that if the $\eta(1440)$ is a $q\bar{q}$ state which decays in a flavor independent way, the partial width relationship between its $\gamma\rho$, and $\gamma\phi$ final states should be $\Gamma_{\gamma\rho} : \Gamma_{\gamma\phi} = 9 : 2$. A simultaneous search for a resonance near 1440 MeV/ c^2 in the $\gamma\rho$ and $\gamma\phi$ mass spectra and a

determination of the branching ratios of the resonance may shed light on the internal structure of the $\eta(1440)$.

Radiative decays of a resonance near 1440 MeV/c² to γV ($V = \rho$, and ϕ) have been studied previously in $J/\psi \rightarrow \gamma\gamma V$ events by Crystal-Ball [6], MarkIII [7] and DM2 [8]. The situation here is further complicated by the proximity of the $f_1(1420)$ to the $\eta(1440)$. MarkIII finds that the 0^- is only slightly favored over the 1^+ in a fit to their angular distributions in $J/\psi \rightarrow \gamma\gamma\rho$ [7].

In this letter, we report a study of decays $J/\psi \rightarrow \gamma\gamma\rho$ and $J/\psi \rightarrow \gamma\gamma\phi$ selected from a sample of 58×10^6 J/ψ events collected by the Beijing Spectrometer (BESII) detector.

2 Event selection

We want to study

$$J/\psi \rightarrow \gamma X, X \rightarrow \gamma V,$$

where X is a resonance, and V denotes vector mesons ρ or ϕ , which are reconstructed via their decays $\rho \rightarrow \pi^+\pi^-$ and $\phi \rightarrow K^+K^-$.

The BESII detector has been described in detail elsewhere [9]. In this study two oppositely charged particles must be detected in the main drift chamber. Photons are detected by the barrel shower counter (BSC) which covers 80% of the 4π solid angle with an energy resolution $\delta E/E = 21\%/\sqrt{E}$. In order to remove electronic noise, the energy deposited in the BSC by each neutral particle is required to have a minimum of 70 MeV. A photon is required to be isolated from charged tracks ($\cos \theta_{\gamma\pi(K)} < 0.98$, where $\theta_{\gamma\pi(K)}$ is the angle between the photon and a charged particle) to reject any photons radiated by a charged particle in the event, and to be consistent with originating from the event interaction point. Photon candidates satisfying these criteria are used for this analysis. The highest energy photon in an event is taken as the radiative photon directly produced in $J/\psi \rightarrow \gamma X$ events.

2.1 Selection of $J/\psi \rightarrow \gamma\gamma\rho \rightarrow \gamma\gamma\pi^+\pi^-$ events

Monte Carlo (MC) simulations have been carried out for both the signal and background processes. The backgrounds considered here are radiative J/ψ decays into two charged tracks, namely $(m\gamma)\pi^+\pi^-$ ($m=1,2,3,4$) and $(n\gamma)K^+K^-$ ($n=1,2,3,4$) for which known branching ratios compiled by the Particle Data Group (PDG)[1] are used to form the correct mixture of these processes in

the Monte Carlo background simulation. The most important backgrounds for this channel are $J/\psi \rightarrow \gamma\eta_c$, $J/\psi \rightarrow \gamma\eta\pi\pi$, $J/\psi \rightarrow \gamma f_1(1510) \rightarrow \gamma\eta\pi\pi$, $J/\psi \rightarrow \omega\pi^0$, $J/\psi \rightarrow \omega\eta$, $J/\psi \rightarrow a_2(1320)\rho$, and $J/\psi \rightarrow b_1^0(1235)\pi^0$. The generated Monte Carlo samples of signal and background are analyzed, and selection variables are varied until an optimized ratio of signal to background is reached. As a result, the following criteria are chosen for the $J/\psi \rightarrow \gamma\gamma\rho \rightarrow \gamma\gamma\pi^+\pi^-$ analysis:

- (1) The sum of momenta of the charged tracks in the event (P_{miss}) is less than $1.14 \text{ GeV}/c$,
- (2) at least one of the two charged tracks in the event must have a higher particle identification confidence level for the pion hypothesis than for the kaon hypothesis by combining the information from TOF and dE/dx ,
- (3) the χ^2 of a four constraint kinematic fit of the event to a $\gamma\gamma\pi^+\pi^-$ topology is less than 10.0,
- (4) the total energy of any photons not used in the kinematic fit in criterion (3) is less than 250 MeV,
- (5) the invariant mass of the two selected photons must be greater than $0.66 \text{ GeV}/c^2$, and
- (6) the helicity angle θ of the dipion in the $\gamma\pi^+\pi^-$ system must satisfy $|\cos\theta| < 0.86$.

Fig. 1 shows the $\pi^+\pi^-$ invariant mass spectrum of the selected $\gamma\gamma\pi^+\pi^-$ events, where a clear ρ signal is visible. To select ρ candidates, $\pi^+\pi^-$ pairs must satisfy $|M_{\pi^+\pi^-} - M_\rho| \leq 0.28 \text{ GeV}/c^2$, as indicated in Fig. 1. Combining the ρ candidate with the lower energy photon in the $\gamma\gamma\pi^+\pi^-$ event, the $\gamma\rho$ mass distribution, shown in Fig. 2, is obtained.

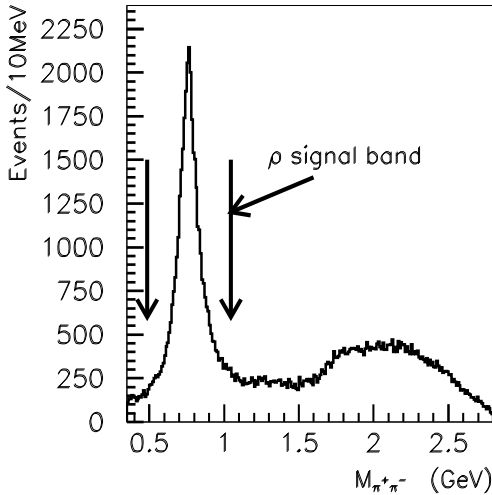


Fig. 1. The $\pi^+\pi^-$ invariant mass distribution.

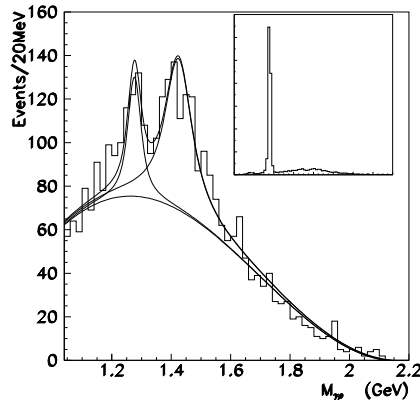


Fig. 2. The $\gamma\rho$ invariant mass distribution. The insert shows the full mass scale where the $\eta(958)$ is clearly observed.

2.2 Selection of $J/\psi \rightarrow \gamma\gamma\phi \rightarrow \gamma\gamma K^+K^-$ events

The selection criteria for $J/\psi \rightarrow \gamma X \rightarrow \gamma\gamma\phi$ ($\phi \rightarrow K^+K^-$) have been chosen in a similar way to those for the $\gamma\gamma\pi^+\pi^-$. According to the Monte Carlo simulation, we find that the major sources of backgrounds are from $J/\psi \rightarrow \phi f_0(980)$, $J/\psi \rightarrow \gamma\eta(1440) \rightarrow \gamma K\bar{K}\pi$, and $J/\psi \rightarrow \gamma f_1(1420) \rightarrow \gamma K\bar{K}\pi$. The final requirements are: $P_{miss} \leq 1.31$ GeV/c, $\chi^2 \leq 25$ for the four constraint kinematic fit to the $J/\psi \rightarrow \gamma\gamma K^+K^-$ hypothesis, and at least one identified charged kaon must be present in the event. The other criteria remain the same for this mode as for the $\gamma\gamma\pi^+\pi^-$ analysis.

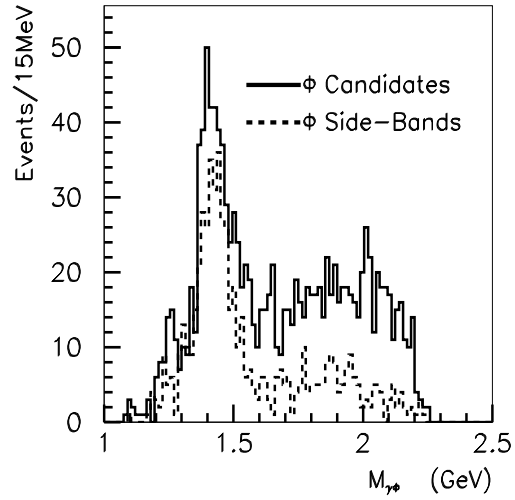
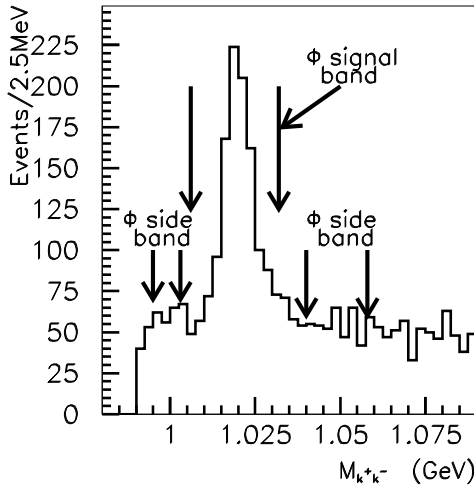


Fig. 3. The K^+K^- invariant mass distribution.

Fig. 4. The $\gamma\phi$ invariant mass distribution.

Fig. 3 shows the K^+K^- mass distribution of the selected events. The ϕ candidates must satisfy $|M_{K^+K^-} - M_\phi| \leq 0.013$ GeV/c². Also shown in Fig. 3 are the side-band regions, as well as the ϕ signal region. The $\gamma\phi$ mass distribution is shown in Fig. 4. The lower energy γ is also combined with the ϕ side-band events forming the dashed distribution, also shown in Fig. 4.

3 Analysis and Results

3.1 $J/\psi \rightarrow \gamma\gamma\rho \rightarrow \gamma\gamma\pi^+\pi^-$ events

We have fitted the mass distributions in Figs. 1 and 3, and estimate that they contain 38249 ± 490 ρ and 764 ± 64 ϕ events, respectively. The insert in Fig. 2 shows the full $\gamma\rho$ mass range, where a strong $J/\psi \rightarrow \gamma\eta'(958) \rightarrow \gamma\gamma\pi^+\pi^-$ signal is observed, as expected. To verify that the mass scale is correct,

we have fitted the $\eta(958)$ signal and obtain 957.5 ± 0.2 MeV/ c^2 for the mass and 0.20 ± 0.04 MeV/ c^2 for the width, which are in excellent agreement with the world average values of 957.78 ± 0.14 MeV/ c^2 and 0.202 ± 0.016 MeV/ c^2 , respectively.

Two enhancements above 1.2 GeV/ c^2 in the $\gamma\rho$ mass spectrum are evident in Fig. 2. We have examined the $\gamma\pi^+\pi^-$ mass distribution for $\pi^+\pi^-$ pairs with masses just above the upper edge of the ρ mass band. The distribution does not exhibit any distinct structures. We conclude that the peaks in Fig. 2 are associated with the ρ .

The identical selection criteria have been applied to a sample of 30 million Monte Carlo inclusive J/ψ events which do not contain the decay $J/\psi \rightarrow \gamma X(1420) \rightarrow \gamma\gamma\rho \rightarrow \gamma\gamma\pi^+\pi^-$. The resulting Monte Carlo $\gamma\pi^+\pi^-$ mass distribution does not show the enhancement at 1420 MeV/ c^2 but does show the $f_1(1285)$, as expected.

In order to extract the resonance parameters in Fig. 2, we perform an unbinned maximum-likelihood fit to the data. The fit function consists of two Breit-Wigner functions, each convoluted with a Gaussian with a mass resolution of 12 MeV/ c^2 , for the signals ($f_1(1285)$ and X(1424)), and a polynomial function for the background. The χ^2/dof of the fit is 68.3/48. In order to check whether the background shape in our fit is correct, we compared it with the background from our J/ψ inclusive MC sample and find that the backgrounds are consistent. The results of the fit are shown in Fig. 2 and summarized in Table 1, where the first errors are statistical errors obtained from the fit and the second are systematic.

The systematic errors on the mass and the width for the first resonance (1276) are determined from the variations when different background functions are used in the fit, about 0.07% and 19.5%, respectively, and from the uncertainty of the Monte Carlo simulation, about 0.6% and 12.5%, respectively. The systematic errors on the mass and the width for the second resonance (1424) include the background function variations, about 0.01% and 2.2%, respectively, and the uncertainty of the Monte Carlo simulation, about 0.8% and 8.4%, respectively.

The detection efficiencies for $J/\psi \rightarrow \gamma X \rightarrow \gamma\gamma\rho \rightarrow \gamma\gamma\pi^+\pi^-$ are determined from a Monte Carlo simulation to be $(9.3 \pm 0.1)\%$ at 1.285 GeV/ c^2 and $(8.81 \pm 0.09)\%$ at 1.420 GeV/ c^2 . The systematic errors on the branching ratios are determined by combining the Monte Carlo uncertainty on the efficiencies (8.4%), the error on the number of J/ψ events (5.0%), and the variation in the number of signal events due to the different background shapes used in the fit (13.2% and 6.5% for the first and second resonances, respectively).

To determine whether the X(1424) is more likely to be the $f_1(1420)$ or the

Table 1

 $J/\psi \rightarrow \gamma X (X \rightarrow \gamma \rho)$ results.

Mass (MeV/c ²)	Width (MeV/c ²)	B($J/\psi \rightarrow \gamma X \rightarrow \gamma \gamma \rho$) ($\times 10^{-4}$)	Events	Signi- ficanc
$1276.1 \pm 8.1 \pm 8.0$	$40.0 \pm 8.6 \pm 9.3$	$0.38 \pm 0.09 \pm 0.06$	203 ± 49	6.3σ
$1424 \pm 10 \pm 11$	$101.0 \pm 8.8 \pm 8.8$	$1.07 \pm 0.17 \pm 0.11$	547 ± 86	9.3σ

$\eta(1440)$, we use the measurement [10] by the WA102 collaboration and PDG results to obtain

$$B(J/\psi \rightarrow \gamma f_1(1420), f_1(1420) \rightarrow \gamma \rho) < 1.7 \times 10^{-5} \text{ (95\% C.L.)}$$

Comparing this limit to our measurement of $B(J/\psi \rightarrow \gamma X(1424) \rightarrow \gamma \gamma \rho) = (1.07 \pm 0.17 \pm 0.11) \times 10^{-4}$, we conclude that of $X(1424)$ in $J/\psi \rightarrow \gamma \gamma \rho^0$ channel should be predominantly $\eta(1440)$.

Table 2

Comparison with other experiments

Decay Mode	Mass (MeV/c ²)	Width (MeV/c ²)	$B(J/\psi \rightarrow \gamma X)^*$ $B(X \rightarrow \gamma V)$ ($\times 10^{-4}$)	Experi- ment
$f_1(1285)$ $\rightarrow \gamma \rho^0$	1281.9 ± 0.6	24.0 ± 1.2	0.34 ± 0.09	PDG [1]
	1271 ± 7	31 ± 14	$0.25 \pm 0.07 \pm 0.03$	MarkIII [7]
	$1276.1 \pm 8.1 \pm 8.0$	$40.0 \pm 8.6 \pm 9.3$	$0.38 \pm 0.09 \pm 0.06$	BESII
$\eta(1440)$ $\rightarrow \gamma \rho^0$	1400-1470	50-80	$0.64 \pm 0.12 \pm 0.07$	PDG [1]
	1432 ± 8	90 ± 26	$0.64 \pm 0.12 \pm 0.07$	MarkIII [7]
	$1424 \pm 10 \pm 11$	$101.0 \pm 8.8 \pm 8.8$	$1.07 \pm 0.17 \pm 0.11$	BESII
$\eta(1440)$ $\rightarrow \gamma \phi$			< 0.82 (95% C.L.)	BESII

For the resonance around 1276 MeV/c², MarkIII [7] finds that the 1^+ hypothesis is preferred over the 0^- by about 4 σ , leading to the conclusion that it is $f_1(1285)$. The BESII results for the mass, width, and branching fraction of the lower mass peak are consistent with those of MarkIII, as shown in Table 2. From MarkIII analysis, it is not distinguishable between 0^- and 1^+ hypothesis for the $X(1432)$ state, but the 0^- slightly better than 1^+ by about 2σ .

3.2 $J/\psi \rightarrow \gamma\gamma\phi \rightarrow \gamma\gamma K^+ K^-$ events

In Fig. 4, the $\gamma\phi$ and $\gamma K^+ K^-$ (ϕ side-bands) distributions are quite similar.

Since the momentum of the charged particles (K^+, K^-) distributed to the (200 MeV/c \sim 800 MeV/c) region in this channel. By combining the information from TOF and dE/dx one can clearly distinguish K from π for charged kaon momenta between 200 MeV/c and 800 MeV/c. Therefore the contamination from π misidentified as K can be neglected.

According to the Monte Carlo simulation, we find that the main backgrounds are as mentioned in Section 2.2. They arise from the decays $J/\psi \rightarrow \phi f_0(980)$, and $J/\psi \rightarrow \gamma\eta(1440) \rightarrow \gamma K \bar{K} \pi$ and $J/\psi \rightarrow \gamma f_1(1420) \rightarrow \gamma K \bar{K} \pi$. These background events are very difficult to reject in our event selection. For these processes a comparison of the two $\gamma K^+ K^-$ invariant mass spectra, derived from the $K^+ K^-$ mass around the ϕ signal and from $K^+ K^-$ from the ϕ side-bands, shows comparable contributions in the $\gamma K^+ K^-$ mass region around 1400 MeV/c². Therefore, the ϕ side-bands can be used to estimate the background in the $\gamma\phi$ spectrum. In Fig. 5 the side-bands subtracted $\gamma\phi$ mass spectrum is shown, and no significant peak around 1420 MeV/c² is observed.

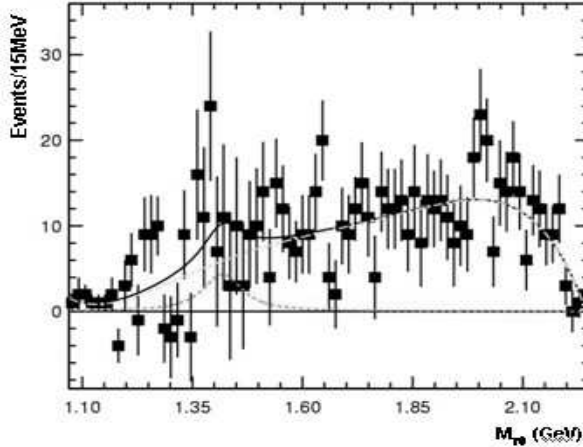


Fig. 5. The invariant mass of $\gamma\phi$ after side-band background subtraction.

A χ^2 fit is performed on the $\gamma\phi$ mass spectrum in Fig. 5. The fit function includes a Breit-Wigner function with mass and width fixed to the values obtained in the fit to the peak at 1420 MeV/c² in Fig. 2, convoluted with a Gaussian with a mass resolution of 12 MeV/c² as predicted by the Monte Carlo simulation, and a polynomial function for backgrounds. The detection efficiency is evaluated from a Monte Carlo simulation of the decay $J/\psi \rightarrow \gamma\gamma\phi$ to be $(5.4 \pm 0.7)\%$. We determine

$$B(J/\psi \rightarrow \gamma X(1424))B(X(1424) \rightarrow \gamma\phi) = (0.31 \pm 0.30) \times 10^{-4}$$

which corresponds to a 95% C. L. upper limit of

$$B(J/\psi \rightarrow \gamma X(1424))B(X(1424) \rightarrow \gamma\phi) < 0.82 \times 10^{-4}$$

Table 2 shows a comparison of results from BESII (this work) and other experiments.

4 Conclusion

If the X(1424) is the lower mass state of the $\eta(1440)$ as mentioned in [1,2], it should be observed in the $J/\psi \rightarrow \gamma\gamma\phi$ channel. Comparing our result on the branching ratio $B(J/\psi \rightarrow \gamma X(1424) \rightarrow \gamma\gamma\rho) = (1.07 \pm 0.17 \pm 0.11) \times 10^{-4}$, and the upper limit of $B(J/\psi \rightarrow \gamma X(1424) \rightarrow \gamma\gamma\phi) < 0.82 \times 10^{-4}$ (95% C.L.), we cannot draw a definite conclusion on whether the X(1424) is either a $q\bar{q}$ state or a glueball state. Therefore, further study is needed to clarify the situation.

5 Acknowledgments

We would like to thank Profs. F.A. Harris, X.C. Lou, D.V. Bugg, H. Yu and Dr. J.D. Richman for valuable discussions.

The BES collaboration thanks the staff of BEPC for their hard efforts. This work is supported in part by the National Natural Science Foundation of China under contracts Nos. 19991480,10225524,10225525, the Chinese Academy of Sciences under contract No. KJ 95T-03, the 100 Talents Program of CAS under Contract Nos. U-11, U-24, U-25, and the Knowledge Innovation Project of CAS under Contract Nos. U-602, U-34(IHEP); and by the National Natural Science Foundation of China under Contract No.10175060(USTC).

References

- [1] K. Hagiwara *et al.*, Phys. Rev. **D66** (2002) 010001
- [2] S. Godfrey and J. Napolitano, Rev. Mod. Phys **71** (1999) 1411
- [3] M. G. Rath *et al.*, Phys. Rev. D40 (1989) 693 ;
A. Bertin *et al.*, Phys. Lett. B361 (1995) 187.
- [4] M. Acciarri *et al.*, Phys. Lett. B501 (2001) 1 ;
F. Close *et al.*, Phys. Rev. D55 (1997) 5749.

- [5] M. S. Chanowitz, Phys. Lett. B164 (1985) 379.
- [6] C. Edwards, PhD thesis, Cal. Tech. Preprint CALT-68-1165 (1985).
- [7] D. Coffman *et al.*, Phys. Rev. D41 (1990) 1410;
J. D. Richman, PhD thesis, Caltech Preprint CALT-68-1231 (1985).
- [8] J. E. Augustin *et al.*, Orsay preprint LAL/85-27 (1985);
J. E. Augustin *et al.*, Phys. Rev. D42 (1990) 10.
- [9] J. Z. Bai *et al.*, Nucl. Instr. Meth. Phys. Res. A344(1994)319;
J. Z. Bai *et al.*, Nucl. Instr. Meth. Phys. Res. A458(2001)627.
- [10] D. Barberis *et al.*, Phys. Lett. B440 (1998) 225.